PERGAMON

International Journal of Heat and Mass Transfer 43 (2000) 2711–2726

International Journal of HEAT and MASS TRANSFER

www.elsevier.com/locate/ijhmt

One-group interfacial area transport of bubbly flows in vertical round tubes

T. Hibiki [a], M. Ishii [b,*]

[a] *Research Reactor Institute, Kyoto University, Kumatori, Sennan, Osaka 590-0494, Japan*
[b] *School of Nuclear Engineering, Purdue University, West Lafayette, IN 47907-1290, USA*

Received 8 January 1999; accepted 14 October 1999

Abstract

In relation to the development of the interfacial area transport equation, the sink and source terms in an adiabatic bubbly flow system were modeled based on the mechanisms of bubble–bubble and bubble–turbulent eddy random collisions, respectively. The interfacial area transport mechanism was discussed based on the derived model. One-dimensional interfacial area transport equation with the derived sink and source terms was evaluated by using the area averaged flow parameters of adiabatic air–water bubbly flows measured in 25.4 mm and 50.8 mm diameter tubes. The flow conditions of the data set covered most of the bubbly flow regime, including finely dispersed bubbly flow (inlet superficial gas velocity: 0.0414–3.90 m/s, superficial liquid velocity: 0.262–5.00 m/s, void fraction: 1.27–46.8%). Excellent agreement was obtained between modeled and measured interfacial area concentrations within the average relative deviation of 11.6%. It was recognized that the present model would be promising for the interfacial area transport of the examined bubbly flows. © 2000 Elsevier Science Ltd. All rights reserved.

Keywords: Interfacial area transport; Two-fluid model; Gas–liquid bubbly flow; Multiphase flow; Internal pipe flow

1. Introduction

In the past twenty-five years, significant developments in the two-phase flow formulation have been accomplished by the introduction of the drift flux model and the two-fluid model. In the present state-of-the-art, the two-fluid model is the most detailed and accurate macroscopic formulation of the thermo-fluid dynamics of two-phase systems. In the two-fluid model, the field equations are expressed by the six conservation equations consisting of mass, momentum and energy equations for each phase. Since these field equations are obtained from an appropriate averaging of local instantaneous balance equations, the phasic interaction term appears in each of the averaged balance equation. These terms represent the mass, momentum and energy transfers through the interface between the phases. The existence of the interfacial transfer terms is one of the most important characteristics of the two-fluid model formulation. These terms determine the rate of phase changes and the degree of mechanical and thermal non-equilibrium between phases, thus they are the essential closure relations which should be modeled accurately. However, because of considerable difficulties ?in terms of measurements and modeling, reliable and accurate closure relations for the interfacial transfer terms are not fully developed.

The geometrical relations developed for the interfacial area concentration [1] show the importance of

* Corresponding author. Tel.: +1-765-494-4587; fax: +1-765-494-9570.

E-mail addresses: hibiki@rri.kyoto-u.ac.jp (T. Hibiki), ishii@ecn.purdue.edu (M. Ishii).

0017-9310/00/$ - see front matter © 2000 Elsevier Science Ltd. All rights reserved.
PII: S0017-9310(99)00325-7

Nomenclature

A	pressure gradient along the flow direction
a_i	interfacial area concentration
$a_{i,0}$	interfacial area concentration at inlet
c	parameter defined by d_e/d_b
D	tube diameter
D_{Sm}	Sauter mean diameter
d_b	bubble diameter
d_e	eddy diameter
$(-dP/dz)_F$	frictional pressure loss
E_B	energy required for breakup
e	energy of a single eddy
F_S	function of c
F_V	function of c
f_B	bubble–eddy random collision frequency
f_C	bubble–bubble random collision frequency
j	mixture volumetric flux
j_g	superficial gas velocity
j_f	superficial liquid velocity
$j_{f,max}$	maximum superficial liquid velocity
K_B	coefficient
K_C	coefficient
k_e	wave number, $2/d_e$
L	tube length
m_e	mass per a single eddy
N_b	number of bubbles
N_e	number of eddies of wave number k_e per volume of liquid
n_b	bubble number density
n_e	number of eddies of wave number per volume of two-phase mixture
P	pressure
r_b	bubble radius
S_B	surface available to the bubble–eddy random collision
S_C	surface available to the bubble–bubble random collision
t	time
t_C	time required for coalescence of bubbles
U_B	volume available to the bubble–eddy random collision
U_C	volume available to the bubble–bubble random collision
u_b	bubble fluctuating velocity
u_B	bubble velocity
u_C	bubble velocity
u_e	eddy velocity
V	control volume
v	particle volume
v_i	interfacial velocity
v_{iz}	z-component of interfacial velocity
z	axial position

Greek symbols

α	void fraction
α_{max}	maximum allowable void fraction
β_B	variable to take account of the overlap of the excluded volume for high void fraction region
β_C	variable to take account of the overlap of the excluded volume for high void fraction region
Γ_B	adjustable valuable
Γ_C	adjustable valuable
γ_B	function of c
γ_C	constant
γ_B	adjustable valuable
γ_C	adjustable valuable
δ_{crit}	critical film thickness where rupture occurs
δ_{init}	initial film thickness
ε	energy dissipation
η	constant of order 1
λ_B	breakup efficiency
λ_C	coalescence efficiency
ρ_f	liquid density
ρ_m	mixture density
σ	interfacial tension
τ_C	contact time for the two bubbles
Φ_j	rate of change of interfacial area concentration due to bubble breakup or coalescence, $(2a_i/3\alpha)\phi_j$
Φ_{Phase}	rate of change of interfacial area concentration due to phase change, $(2a_i/3\alpha)\phi_{Phase}$
$\Phi_{Pressure}$	rate of change of interfacial area concentration due to pressure change
Φ_{RC}	rate of increase of interfacial area concentration due to bubble random collision
Φ_{Sink}	rate of decrease of interfacial area concentration due to bubble coalescence
Φ_{Source}	rate of increase of interfacial area concentration due to bubble breakup
Φ_{TI}	rate of increase of interfacial area concentration due to turbulent impact
ϕ_j	rate of change of interfacial area concentration due to bubble breakup or coalescence
ϕ_{Phase}	rate of change of interfacial area concentration due to phase change
ψ	factor depending on the shape of the bubbles

Subscripts

calc.	calculated value
meas.	measured value
0	value at inlet

Mathematical symbols

$\langle\rangle$	cross-sectional area averaging quantity
$\langle\langle\rangle\rangle$	void fraction weighted cross-sectional area averaging quantity
$\langle\langle\rangle\rangle_a$	interfacial area concentration weighted cross-sectional area averaging quantity

the existence and size of small fluid particles for all flow regimes. For example, the maximum stable bubble size, mechanisms of bubble coalescence, disintegration and nucleation are important for bubbly, slug and churn flows. In order to accurately predict the interfacial area concentration for these flow regimes, it may be necessary to introduce a transport equation for the interfacial area [2]. For example, for a boiling flow, a bubble number transport equation can be written in terms of the bulk liquid bubble nucleation rate, the bubble number density sink rate due to coalescence and collapse, and generation rate due to bubble disintegration [3]. This equation is equivalent to the interfacial area transport equation.

Since the interfacial area concentration changes with the variation of the particle number density due to coalescence and breakage, analogous to Boltzman's transport equation, a Population Balance Approach (PBA) was recently proposed by Reyes [4] to develop a particle number density transport equation for chemically non-reacting, dispersed spherical fluid particles. For the purpose to take account of interfacial area transport, Kocamustafaogullari and Ishii [5] generalized Reyes's model, then taking a moment of number density with interfacial area, they obtained the interfacial area transport equation based on statistical mechanics. The simplest form of the interfacial area transport equation can be obtained by applying the cross-sectional area averaging and reducing it to a one-dimensional form. This form of the interfacial area transport equation may have the most useful and practical applications in the existing one-dimensional two-fluid model. It can replace the traditional flow regime maps and regime transition criteria. The changes in the two-phase flow structure are predicted mechanistically by introducing the interfacial area transport equation. The effects of the boundary conditions and flow development are efficiently modeled by this transport equation. Such a capability does not exist in the current state-of-the-art. Thus, a successful development of the interfacial area transport equation can make a quantum improvement in the two-fluid model formulation.

The transport equation requires several constitutive relations to model the fluid particle coalescence and disintegration. The development of the source and sink terms in the transport equation heavily depends on understanding the mechanisms of particle coalescence and disintegration as well as accurate experimental data for the changes in the interfacial area in two-phase flow. Some phenomenological models for the sink and source terms have been proposed based on the mechanism for fluid particle coalescence and disintegration [6–9]. Recently, Wu and Ishii [10,11] proposed the general approach to treat the bubbles in two groups: the spherical/distorted bubble group and the cap/slug bubble group, resulting in two bubble number density transport equations that involve the inner and inter group interactions. In their study the mechanisms of these interactions was summarized in five categories: the coalescence due to random collisions driven by turbulence, the coalescence due to wake entrainment, the breakage due to the impact of turbulent eddies, the shearing-off of small bubbles from cap bubbles, and the breakage of large cap bubbles due to flow instability on the bubble surface. They reduced the two-group transport equations to one-group for a bubbly flow with relatively low void fraction and developed the model of the source and sink terms. The obtained one-group interfacial area transport equation was examined by some existing data of bubbly flow in low void fraction region [12]. Although sink and source terms due to bubble coalescence and breakup were appropriately formulated in their study, the gas phase was assumed to be incompressible without phase change [10,11]. It turned out from recent studies by the present authors [13–15] that the increase of the interfacial area concentration due to pressure reduction along the flow direction could not be ignored for a vertical gas–liquid bubbly flow and the data set used in their study [10,11] was not accurate enough to be used for verification of modeled sink and source terms [13]. Therefore, their data analysis method needs to be improved and the contribution of sink and source terms to the interfacial area transport should be reexamined based on an accurate data set. Städtke et al. [16] also modeled the source and sink terms in the interfacial area transport equation and tested the model with the JRC Ispra code for 2D inhomogeneous two-phase flow. However, it has been difficult to validate the models over a wide range of flow conditions, since little rigorous data set has been available.

Recently, a complete set of data on local void fraction, interfacial area concentration, interfacial velocity, bubble size, liquid velocity, and turbulence intensity was taken at the Thermal-hydraulics and Reactor Safety Laboratory in Purdue University by using the local sensors such as the double sensor probe and hot-film probe over a wide range of bubbly flow conditions in 25.4 and 50.8 mm diameter tubes [13–15]. The purpose of this study is to develop source and sink terms in the interfacial area transport equation for adiabatic bubbly flows and to validate developed model by the data set.

2. Model development of bubble coalescence and breakage

2.1. Interfacial area transport equation

Kocamustafaogullari and Ishii [5] derived the interfacial area transport equation from the statistical model of fluid particle number transport equation as follows. They obtained the fluid particle number density transport equation of particles having volume v by a simple procedure accounting for the fluid particle entering and leaving a control volume through different mechanisms under the assumption of a continuous particle density distribution function. The interfacial area concentration transport equation of particles of volume v was derived by multiplying the particle number density transport equation of particles having volume v by the average interfacial area of particles of volume v, which was independent of the spatial coordinate system. Since the fluid particle interfacial area concentration transport equation of volume v was much too detailed for practical purposes, they developed an interfacial area transport equation averaged over all particle sizes by integrating the equation from minimum particle volume to the maximum possible particle volume. The resulting equation includes the source and sink terms due to the particle interactions, interfacial phase change, and compressibility of fluid particle [5,10,11]

$$\begin{aligned}&\frac{\partial a_i}{\partial t}+\nabla\cdot a_i\vec{v}_i=\frac{1}{3\psi}\left(\frac{\alpha}{a_i}\right)^2\left[\sum_j\phi_j+\phi_{\text{Phase}}\right]\\&+\left(\frac{2a_i}{3\alpha}\right)\left[\frac{\partial\alpha}{\partial t}+\nabla\cdot\left(\vec{v}_i\alpha\right)\right]=\left[\sum_j\Phi_j+\Phi_{\text{Phase}}\right]\\&+\left(\frac{2a_i}{3\alpha}\right)\left[\frac{\partial\alpha}{\partial t}+\nabla\cdot\left(\vec{v}_i\alpha\right)\right]=\sum_j\Phi_j+\Phi_{\text{Phase}}+\Phi_{\text{Pressure}}\end{aligned}\tag{1}$$

where a_i, t, $\vec{v}_i$, ψ, α, ϕ_j and ϕ_{Phase} denotes the interfacial area concentration, the time, the interfacial velocity, the factor depending on the shape of the bubbles, the void fraction, the rate of change of interfacial area concentration due to bubble breakup or coalescence, and the rate of change of interfacial area concentration due to phase change, respectively. For spherical bubbles, ψ equals $1/(36\pi)$.

By applying the cross-sectional area averaging, the one-dimensional interfacial area transport equation becomes:

$$\begin{aligned}&\frac{\partial\langle a_i\rangle}{\partial t}+\frac{\partial}{\partial z}(\langle a_i\rangle\langle\langle v_{iz}\rangle\rangle_a)\\&=\langle\Phi_{\text{Source}}\rangle-\langle\Phi_{\text{Sink}}\rangle+\langle\Phi_{\text{Phase}}\rangle+\langle\Phi_{\text{Pressure}}\rangle\end{aligned}\tag{2}$$

where the brackets of $\langle\ \rangle$ and $\langle\langle\ \rangle\rangle_a$ mean the cross-sectional area averaging quantity and the interfacial area concentration weighted cross-sectional area averaging quantity, respectively. Under the adiabatic and steady conditions, there are no effects of phase changes; thus:

$$\frac{\mathrm{d}}{\mathrm{d}z}(\langle a_i\rangle\langle\langle v_{iz}\rangle\rangle_a)=\langle\Phi_{\text{Source}}\rangle-\langle\Phi_{\text{Sink}}\rangle+\langle\Phi_{\text{Pressure}}\rangle\tag{3}$$

Ishii et al. [5,10,11] classified the source and sink terms into five basic mechanisms, namely random collision of bubbles and wake entrainment for the sink terms, and turbulent impact, shearing-off and interfacial instability for the source terms. Among them, wake entrainment would play an important role in the bubbly flow condition near the bubbly to slug flow transition boundary, and the slug flow. It may be also important for the bubbly flow in a small diameter tube, and very low flow conditions as the lateral fluctuation velocity of bubbles is small. However, for relatively high flow conditions, even bubbles captured in the wake region would easily left the region due to liquid turbulence, resulting in a minor contribution of wake entrainment to the interfacial area transport. Shearing-off and interfacial instability would become important for relatively large bubbles, which appear in the bubbly flow condition near the bubbly to slug flow transition boundary, and the slug flow. Since this study focuses on the development of one-group interfacial area transport equation in a bubbly flow, random collision of bubbles for the sink term, and turbulent impact for the source term are considered as main mechanisms of the interfacial area transport.

2.2. Modeling of bubble coalescence

The bubble coalescence is considered to occur due to the bubble random collision induced by turbulence in a liquid phase. For the estimation of bubble–bubble collision frequency, it is assumed that the movement of bubbles behaves like ideal gas molecules [6]. Following the kinetic theory of gases [17], the bubble random col-

lision frequency f_C can be expressed by assuming the same velocity of bubbles $\overline{u_C}$ as a function of surface available to the collision S_C, and volume available to the collision U_C:

$$f_C = \frac{\overline{u_C} S_C}{4 U_C} \tag{4}$$

Taking account of the excluded volume for bubbles, the surface and volume are given by:

$$S_C = 4\pi(N_b - 1)d_b^2 \cong 4\pi N_b d_b^2 = V\frac{24\alpha}{d_b} \tag{5}$$

$$U_C = V\left(1 - \beta_C \frac{2}{3}\pi n_b d_b^3\right) = 4\beta_C V(\alpha_{max} - \alpha), \quad \alpha_{max} \equiv \frac{1}{4\beta_C} \tag{6}$$

where N_b, d_b, V, and α denote the number of bubbles, the bubble diameter, the control volume, and the void fraction, respectively. The variable β_C (≤ 1) is introduced into the excluded volume in order to take account of the overlap of the excluded volume for high void fraction region. Although it may be a function of the void fraction, it is treated as a constant for simplicity. The distortion caused by this assumption will be adjusted by a tuning parameter in a final equation of the bubble coalescence rate as introduced later.

The mean fluctuation velocity difference between two points being apart by d_b in the inertial subrange of isotropic turbulence is given by [18]

$$\overline{u_b} = 1.4(\varepsilon d_b)^{1/3} \tag{7}$$

where ε denotes the energy dissipation. Taking account of the relative motion between bubbles, the average bubble velocity is given by:

$$\overline{u_C} = \gamma_C(\varepsilon d_b)^{1/3} \tag{8}$$

where γ_C is a constant. The value of ε is simply obtained from the mechanical energy equation [19] as:

$$\varepsilon = \frac{\langle j \rangle}{\rho_m}\left(-\frac{dP}{dz}\right)_F \tag{9}$$

where j, ρ_m, and $(-dP/dz)_F$ denote the mixture volumetric flux, the mixture density, and the gradient of the frictional pressure loss along the flow direction, respectively. The collision frequency will increase to infinity, as the void fraction approaches to maximum void fraction calculated by closed packing condition. Following Taitel et al. [20], the maximum allowable void fraction α_{max} is determined to be 0.52, which gives the finely dispersed bubbly to slug flow transition boundary. Finally, one obtains

$$f_C = \frac{\gamma_C' \alpha \varepsilon^{1/3}}{d_b^{2/3}(\alpha_{max} - \alpha)} \tag{10}$$

where γ_C' is an adjustable valuable.

In order to obtain the bubble coalescence rate, it is necessary to determine a coalescence efficiency. Coulaloglou and Tavlarides [6] gave an expression for the coalescence efficiency λ_C as a function of a time required for coalescence of bubbles t_C and a contact time for the two bubbles τ_C:

$$\lambda_C = \exp\left(-\frac{t_C}{\tau_C}\right) \tag{11}$$

The time required for coalescence of bubbles was given by Oolman and Blanch [21,22] for the thinning of the liquid film between bubbles of equal size as:

$$t_C = \frac{1}{8}\sqrt{\frac{\rho_f d_b^3}{2\sigma}} \ln\frac{\delta_{init}}{\delta_{crit}} \tag{12}$$

where ρ_f, σ, δ_{init}, and δ_{crit} mean the liquid density, interfacial tension, the initial film thickness, and the critical film thickness where rupture occurs. Kirkpatrick and Locket [23] estimated the initial thickness of the film in air–water systems to be 1×10^{-4} m, whereas the final film thickness was typically taken as 1×10^{-8} m [24]. On the other hand, Levich [25] derived the contact time in turbulent flows from dimensional consideration.

$$\tau_C = \frac{r_b^{2/3}}{\varepsilon^{1/3}} \tag{13}$$

where r_b means the bubble radius. Finally, one obtains:

$$\lambda_C = \exp\left(-K_C \sqrt[6]{\frac{d_b^5 \rho_f^3 \varepsilon^2}{\sigma^3}}\right) \tag{14}$$

where K_C (= 1.29) denotes the coefficient.

The final form of the bubble coalescence rate Φ_{RC} is expressed as:

$$\Phi_{RC} = \frac{1}{3\psi}\left(\frac{\alpha}{a_i}\right)^2 \cdot f_C \cdot n_b \cdot \lambda_C = \left(\frac{\alpha}{\alpha_i}\right)^2 \frac{\Gamma_C \alpha^2 \varepsilon^{1/3}}{d_b^{11/3}(\alpha_{max} - \alpha)} \exp\left(-K_C \sqrt[6]{\frac{d_b^5 \rho_f^3 \varepsilon^2}{\sigma^3}}\right) \tag{15}$$

where Γ_C is an adjustable valuable, which is determined experimentally to be 0.188 for a bubbly flow.

2.3. Modeling of bubble breakup

The bubble breakup is considered to occur due to the collision of the turbulent eddy with the bubble. For the estimation of bubble–eddy collision frequency, it is assumed that the movement of eddies and bubbles behaves like ideal gas molecules [6]. Furthermore, the following assumptions are made for the modeling of the bubble–eddy collision rate [7]: (i) the turbulence is isotropic; (ii) the eddy size d_e of interest lies in the inertial subrange; (iii) the eddy with the size from cd_b to d_b can break up the bubble with the size of d_b, since larger eddies have the tendency to transport the bubble rather than to break it and smaller eddies do not have enough energy to break it. Azbel and Athanasios [26] developed the following expression for the number of eddies as a function of wave number.

$$\frac{dN_e(k_e)}{dk_e} = 0.1k_e^2 \tag{16}$$

where $N_e(k_e)$ denotes the number of eddies of wave number $k_e\,(=2/d_e)$ per volume of fluid. Here, the number of eddies of wave number per volume of two-phase mixture $n_e(k_e)$ is given by:

$$n_e(k_e) = N_e(k_e)(1-\alpha) \tag{17}$$

Following the kinetic theory of gases [17], the bubble–eddy random collision frequency f_B can be expressed by assuming the same velocity of bubbles $\overline{u_B}$ as a function of the surface available to the collision S_B, and the volume available to the collision U_B:

$$f_B = \frac{\overline{u_B} S_B}{4U_B} \tag{18}$$

Taking account of the excluded volume for the bubbles and eddies, the surface and volume are given by:

$$\begin{aligned} S_B &= \int 4\pi(N_b - 1)\left(\frac{d_b}{2} + \frac{d_e}{2}\right)^2 dn_e \Big/ \int dn_e \\ &= 4\pi N_b d_b^2 \cdot F_S(c) = V\frac{24\alpha}{d_b}F_S(c) \end{aligned} \tag{19}$$

$$\begin{aligned} U_B &= V\left(1 - \beta_B \int \frac{2}{3}\pi n_b \left(\frac{d_b}{2} + \frac{d_e}{2}\right)^3 dn_e \Big/ \int dn_e\right) \\ &= V\left(1 - \beta_B \frac{2}{3}\pi n_b d_b^3 \cdot F_V(c)\right) \\ &= 4\beta_B F_V(c) V(\alpha_{max} - \alpha) \end{aligned} \tag{20}$$

where $F_S(c)$ and $F_V(c)$ are functions of c defined by d_e/d_b. The variable $\beta_B\,(\le 1)$ is introduced into the excluded volume in order to take account of the overlap of the excluded volume for high void fraction region. Although it may be a function of the void fraction, it is treated as a constant for simplicity. The distortion caused by this assumption will be adjusted by a tuning parameter in a final equation of the bubble breakup rate as introduced later.

According to Kolmogorov's law [27], for the inertial subrange of the energy spectrum, the eddy velocity u_e is given as:

$$u_e^2 = 8.2(\varepsilon/k_e)^{2/3} \quad \text{or} \quad u_e = 2.3(\varepsilon d_e)^{1/3} \tag{21}$$

Here, taking account of the relative motion between bubble and eddy with the same size of bubble, the averaged relative velocity $\overline{u_B}$ can be expressed as:

$$\overline{u_B} = \gamma_B(c)(\varepsilon d_b)^{1/3} \tag{22}$$

where $\gamma_B(c)$ is a function of c. Finally, one obtains

$$f_B = \frac{\gamma_B'(c)\alpha\varepsilon^{1/3}}{d_b^{2/3}(\alpha_{max} - \alpha)} \tag{23}$$

where $\gamma_B'(c)$ is an adjustable valuable.

In order to obtain the bubble breakup rate, it is necessary to determine a breakup efficiency. Following Tsouris and Tavlarides [9], the energy of a single eddy is given by:

$$e = \frac{1}{2}m_e u_e^2 = 0.43\pi\rho_f d_e^{11/3}\varepsilon^{2/3} \tag{24}$$

where m_e means the mass per a single eddy. Considering bubble breakup into two equal-size bubbles, the energy required for breakup E_B is calculated as follows:

$$E_B = 2\pi\sigma\left(\frac{d_b}{2^{1/3}}\right)^2 - \pi\sigma d_b^2 = 0.587\pi\sigma d_b^2 \tag{25}$$

The breakup efficiency λ_B is then assumed to be given by the following exponential function [6,7,9]:

$$\begin{aligned} \lambda_B &= \exp\left(-\frac{E_B}{\eta e}\right) = \exp\left(-\frac{1.37}{\eta c^{11/3}} \cdot \frac{\sigma}{\rho_f d_b^{5/3}\varepsilon^{2/3}}\right) \\ &= \exp\left(-K_B \cdot \frac{\sigma}{\rho_f d_b^{5/3}\varepsilon^{2/3}}\right) \end{aligned} \tag{26}$$

where η is a constant of order 1 [9]. K_B value for the average breakup efficiency is simply calculated by setting $c = d_e/d_b = 1$ to be 1.37. The final form of the bubble breakup rate Φ_{TI} is expressed as:

$$\begin{aligned} \Phi_{TI} &= \frac{1}{3\psi}\left(\frac{\alpha}{a_i}\right)^2 \cdot f_B \cdot n_e \cdot \lambda_B \\ &= \left(\frac{\alpha}{\alpha_i}\right)^2 \frac{\Gamma_B \alpha(1-\alpha)\varepsilon^{1/3}}{d_b^{11/3}(\alpha_{max} - \alpha)} \exp\left(-\frac{K_B\sigma}{\rho_f d_b^{5/3}\varepsilon^{2/3}}\right) \end{aligned} \tag{27}$$

Table 1
Dimensions of experimental loops

Loop	Loop (A)	Loop (B)
Tube inner diameter, D	25.4 mm	50.8 mm
Tube length, L	3750 mm	3061 mm
Axial measuring station, z/D	12.0, 65.0, 125	6.00, 30.3, 53.5
Air injection method	Porous tube (40 μm)	Porous tube (40 μm)
Pump power (maximum superficial liquid velocity)	~4 m/s	~10 m/s
Air supply system	9.91 m^3 air tank pressurized to 0.929 MPa	

where Γ_B is an adjustable valuable, which is determined experimentally to be 0.264 for a bubbly flow.

3. Results and discussion

3.1. Data base used for evaluation of derived model

In order to evaluate the derived model of sink and source terms in the interfacial area transport equation, the authors measured local flow parameters of adiabatic air–water bubbly flows in vertical round tubes at the Thermal-hydraulics and Reactor Safety Laboratory in Purdue University [13–15]. The dimensions of the loops used in the experiments are shown in Table 1. Local measurements of void fraction, interfacial area concentration, interfacial velocity, and Sauter mean diameter were performed by using the double sensor probe method [13,28]. On the other hand, local measurements of liquid velocity and turbulence intensity were conducted by using hotfilm anemometry [13]. The instruments such as a conductivity probe and a hotfilm probe were held and positioned along the radius of the tube using a traversing mechanism which mounted directly to the tube flange. Data was taken at three different axial locations as well as fifteen radial positions. One-dimensional flow parameters, that is, area averaged quantities can be obtained by integrating the local flow parameters over the flow channel. In order to verify the measurement accuracy, obtained one-dimensional flow parameters were compared with those measured by other cross-calibration methods. Good agreements were obtained between the area averaged void fraction, interfacial area concentration and Sauter mean diameter, the interfacial gas velocity and liquid velocity obtained from the local measurements, and those measured by the γ-densitometer, the photographic method, the rotameter, and the magnetic flow meter within the error of 5.74, 6.95, 12.4 and 5.19%, respectively [13,14].

Flow conditions of the experiments are listed in Tables 2 and 3. The conditions are also shown in Fig. 1(a) and (b). The flow conditions cover most of the bubbly flow regime, including finely dispersed bubbly flow. The solid and broken lines in Fig. 1(a) and (b) indicate the flow regime transition boundaries predicted by the model of Taitel et al. [20] and the phase distribution pattern boundaries given by Serizawa and Kataoka [29], respectively.

3.2. Predictions of flow parameters used in interfacial area transport calculation

In order to perform the interfacial area transport calculation, local pressure, superficial gas velocity, gas velocity (or z-component of the interfacial velocity), void fraction, gas velocity weighted by the interfacial area concentration, and Sauter mean diameter should

Table 2
Flow conditions in the experiment using a 25.4 mm diameter tube [15][a]

Symbols	○	△	□	▽	◇
j_f (m/s)	$j_{g,0}$ (m/s)	$j_{g,0}$ (m/s)	$j_{g,0}$ (m/s)	$j_{g,0}$ (m/s)	$j_{g,0}$ (m/s)
0.262	0.0549 (13.7)	0.0610 (15.4)	0.0780 (19.2)	0.0990 (23.2)	0.117 (26.6)
0.872	0.0414 (5.09)	0.0813 (9.35)	0.143 (15.2)	0.210 (20.6)	0.305 (26.8)
1.75	0.0461 (3.14)	0.116 (7.31)	0.257 (14.4)	0.399 (19.7)	0.575 (25.2)
2.62	0.0804 (3.56)	0.193 (7.87)	0.401 (14.6)	0.581 (19.7)	0.764 (24.2)
3.49	0.0509 (1.83)	0.201 (6.57)	0.516 (15.1)	0.702 (19.5)	0.931 (24.2)

[a] Values in the parentheses indicate the void fractions in % measured at $z/D = 125$.

Table 3
Flow conditions in the experiment using a 50.8 mm diameter tube [14][a]

Symbols	○	△	□	▽	◇	*
j_f (m/s)	$j_{g,0}$ (m/s)	$j_{g,0}$ (m/s)	$j_{g,0}$ (m/s)	$j_{g,0}$ (m/s)	$j_{g,0}$ (m/s)	$j_{g,0}$ (m/s)
0.491	0.0275 (4.90)	0.0556 (9.20)	0.129 (19.2)	0.190 (25.9)	N/A	N/A
0.986	0.0473 (5.12)	0.113 (10.8)	0.242 (20.3)	0.321 (23.1)	N/A	N/A
2.01	0.103 (5.68)	0.226 (10.8)	0.471 (18.3)	0.624 (22.8)	N/A	N/A
5.00	0.245 (5.41)	0.518 (10.6)	1.11 (20.0)	1.79 (28.1)	2.87 (36.6)	3.90 (44.2)

[a] Values in the parentheses indicate the void fractions in % measured at $z/D = 53.5$.

be given by either a constitutive relation or a measured value. For example, the system pressure can be calculated by using Lockhart–Martinelli's method [30] to estimate the two-phase frictional pressure loss. Good agreement was obtained between calculated and measured system pressures within the averaged relative error of 0.99% (maximum relative error of 5.04%) in the experiment. The drift flux model [31] can be used for the predictions of the void fraction and the gas velocity. The predicted gas velocities agreed with ones measured in the experiments within the averaged relative error of 11.3%.

To examine the validity of the modeled sink and source terms, flow parameters used in the calculation should be as accurate as possible. Therefore, the empirical equations shown in Table 4 are used in this calculation. The functional form of the system pressure is obtained from the linear pressure reduction along the flow direction in the measured range. The functional form of the void fraction is determined from insignificant change of gas velocity along the flow direction (less than 3%). In the equations, P_0, $\langle j_{g,0}\rangle$, $\langle \alpha_0 \rangle$, and A mean the inlet pressure, the inlet superficial gas velocity, the inlet void fraction, and the pressure gradient along the flow direction, respectively. These values were determined by values measured at three axial locations. Table 5 shows typical values used in the interfacial area transport calculations to be presented in the next section. The expected estimation errors are also shown in Fig. 2 and Table 4. The empirical equations give better estimations of the pressure and the gas velocity rather than the models such as the Lockhart–Martinelli's equation and the drift flux model.

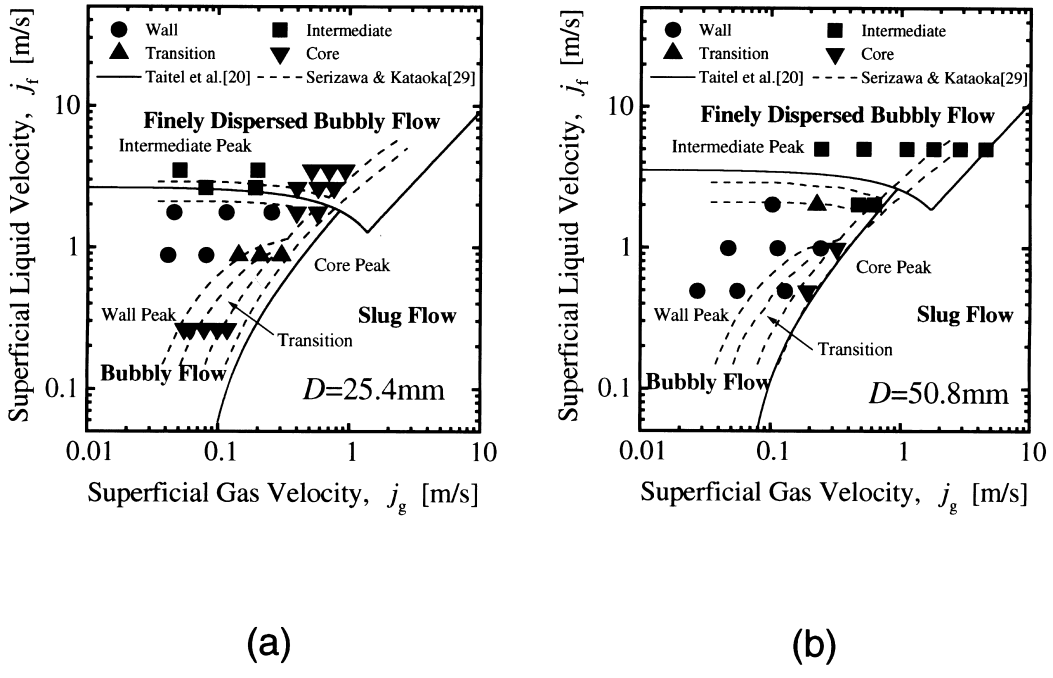

Fig. 1. Flow conditions in the experiments using 25.4 mm and 50.8 mm diameter tubes.

Table 4
Empirical correlations used in the predictions of system pressure and flow parameters

Quantities	Empirical correlations	Prediction accuracy
System pressure	$P = \{P_0 + A \cdot (z/D)\}$	$< 0.5\%$ (Max.: $< 1\%$)
Superficial gas velocity	$\langle j_g \rangle = \dfrac{\langle j_{g,0} \rangle \cdot P_0}{P}$	10.2%
Void fraction	$\langle \alpha \rangle = \dfrac{\langle \alpha_0 \rangle \cdot P_0}{P}$	9.64%
Gas velocity (interfacial velocity)	$\langle\langle v_g \rangle\rangle = \dfrac{\langle j_g \rangle}{\langle \alpha \rangle} = \dfrac{\langle j_{g,0} \rangle}{\langle \alpha_0 \rangle} = \langle\langle v_{g,0} \rangle\rangle$	2.93%
Gas velocity weighted by interfacial area concentration	$\langle\langle v_{gz} \rangle\rangle_a \equiv \dfrac{\langle v_{gz} a_i \rangle}{\langle a_i \rangle} \approx \dfrac{\langle v_{gz} \alpha \rangle}{\langle \alpha \rangle} = \langle\langle v_g \rangle\rangle$	1.40%

The interfacial area concentrations measure at the first measuring station such as $z/D = 12.0$ for $D = 25.4$ mm or $z/D = 6.00$ for $D = 50.8$ mm are used as initial values. It should be noted here that the accuracy of the initial value may affect the final result of the calculation on the order of the accuracy of the initial value. The Sauter mean diameters are calculated by the following relation:

$$\langle D_{\mathrm{Sm}} \rangle = \frac{6\langle \alpha \rangle}{\langle a_i \rangle} \tag{28}$$

Here, due to the spherical bubble assumption, we set $\langle d_b \rangle \approx \langle D_{\mathrm{Sm}} \rangle$ in this calculation. Since the uniform bubble size is assumed, the area-averaged bubble interfacial velocity weighted by interfacial area concentration can be given by [11]:

$$\langle\langle v_{iz} \rangle\rangle_a \equiv \frac{\langle v_{iz} a_i \rangle}{\langle a_i \rangle} \approx \frac{\langle v_{iz} \alpha \rangle}{\langle \alpha \rangle} = \langle\langle v_{iz} \rangle\rangle \tag{29}$$

where the bracket of $\langle\langle\rangle\rangle$ means the void fraction weighted cross-sectional area averaging quantity. As shown in Fig. 2 and Table 4, the area-averaged bubble interfacial velocities weighted by interfacial area concentration agree with those weighted by void fraction within the average relative deviation of 1.40%.

Since measured values of the frictional pressure loss are not available, the Lockhart–Martinelli's method [30] with Chisholm's equation [32] is used to estimate the two-phase frictional pressure loss in the calculation of the energy dissipation given by Eq. (9). The prediction error of this model will be adjusted by the adjustable valuables, Γ_B and Γ_C.

3.3. Contributions of bubble coalescence, breakup and expansion to interfacial area transport

In order to evaluate the contributions of bubble coalescence, breakup and expansion to interfacial area transport, typical changes of interfacial area concentration due to each mechanism along axial position are shown in Figs. 3–5. The changes of the system pressure, the void fraction and the Sauter mean diameter along the flow direction are also shown in Fig. 6. In these figures, measured values are indicated by open symbols.

For the case of low liquid velocity and low void fraction such as $j_f = 0.491$ m/s and $j_{g,0} = 0.0275$ m/s ($\alpha_{z/D=53.5} = 4.90\%$), the change of the interfacial area

Table 5
Typical initial values used in the interfacial area transport calculation

Quantities	Case I	Case II	Case III
Inlet superficial gas velocity, $\langle j_{g,0} \rangle$ (m/s)	0.0275	0.190	3.90
Superficial liquid velocity, $\langle j_f \rangle$ (m/s)	0.491	0.491	5.00
Inlet pressure, P_0 (MPa)	0.133	0.127	0.170
Pressure gradient, A (MPa)	−0.000522	−0.000406	−0.000754
Inlet void fraction, $\langle \alpha_0 \rangle$	0.0376	0.220	0.357
Interfacial area concentration, $\langle a_{i,\, z/D=6.00} \rangle$ (m^{-1})	92.9	408	779
Sauter mean diameter, $\langle D_{\mathrm{Sm},\, z/D=6.00} \rangle$ (mm)	2.49	3.31	2.83

concentration predicted by the derived model suggests that bubble coalescence due to random collision between bubbles (bubble random collision) and bubble breakup due to random collision between bubble and turbulent eddy (turbulent impact) are not marked (see Fig. 3). For this flow condition, the bubble mixing length may not be large enough to cause the bubble random collision because of long distance between bubbles. Fig. 7 shows the bubble coalescence and breakup efficiency predicted by the models. For the small turbulence fluctuation, the bubble contact time is relatively long, resulting in high coalescence efficiency ($\lambda_C \sim 0.96$), whereas the turbulent eddy may not have enough energy to disintegrate the bubbles ($\lambda_B \sim 0$). This leads to a major role of the bubble expansion due to pressure reduction along axial direction in the interfacial area transport. As a result, the interfacial area concentration increases along axial direction mainly due to the pressure reduction. Reasonably good agreement is obtained between predicted and measured interfacial area concentrations.

For the case of low liquid velocity and high void fraction such as $j_f = 0.491$ m/s and $j_{g,0} = 0.190$ m/s ($\alpha_{z/D=53.5} = 25.9\%$), the increase of void fraction would enhance the rate of collision between bubbles as well as that between bubble and turbulent eddy. The enhancement of the bubble coalescence along the flow direction tends to decrease the interfacial area concentration along the flow direction. On the other hand, the increase rate of the bubble breakup due to turbulent impact is not marked because of the gradual decrease of eddy number with increasing void fraction, and the low bubble breakup efficiency ($\lambda_B \sim 0$) as shown in Fig. 7. As a consequence, the increase of the interfacial area concentration along the flow direction is smaller than that expected by the bubble expansion.

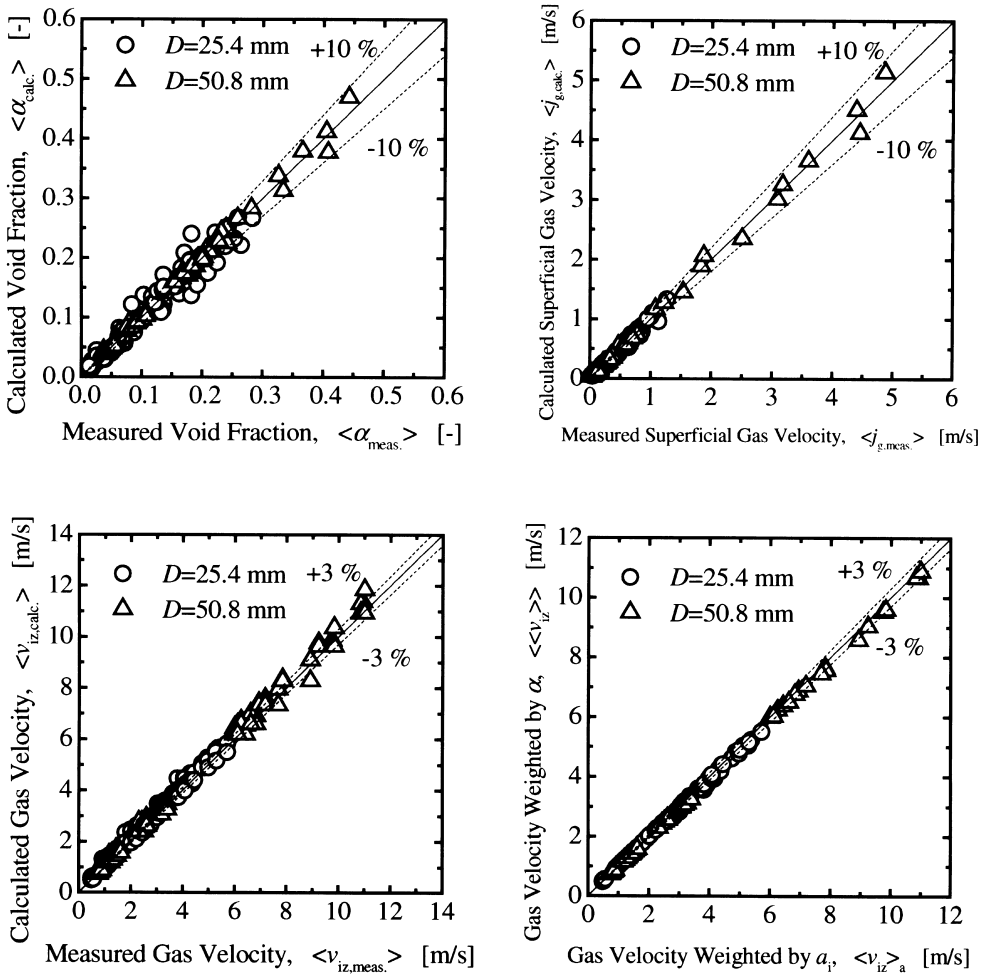

Fig. 2. Verification of empirical correlations used in the calculations of void fraction, superficial gas velocity, gas velocity, and gas velocity weighted by interfacial area concentration.

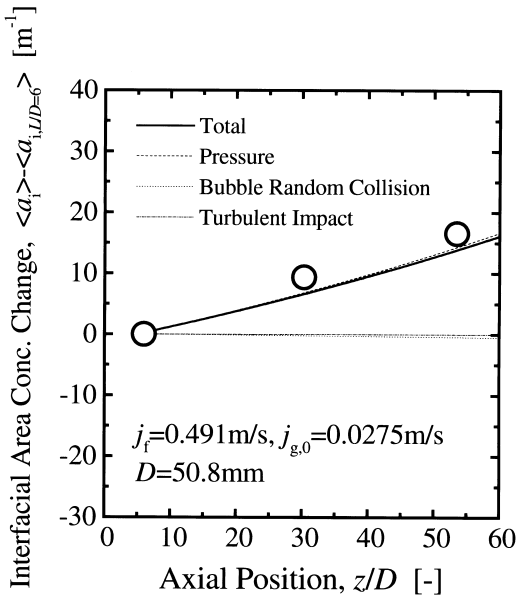

Fig. 3. Contributions of bubble coalescence, breakup and expansion to interfacial area transport ($j_f = 0.491$ m/s, $j_{g,0} = 0.0275$ m/s).

For a finely dispersed bubbly flow condition such as $j_f = 5.00$ m/s and $j_{g,0} = 3.90$ m/s ($\alpha_{z/D=53.5} = 44.2\%$), the strong turbulence disintegrates bubbles into small bubbles, resulting in the increase of the high interfacial area concentration (See Fig. 5). As can be seen in Fig. 7, the strong turbulence increases the bubble breakup efficiency significantly ($\lambda_B \sim 0.92$). On the other hand, the large turbulence fluctuation may decrease the bubble contact time, resulting in the decrease of the bubble coalescence efficiency ($\lambda_C \sim 0.6$). Consequently, the bubble breakup rate becomes higher than the bubble coalescence rate. The increase of the interfacial area concentration along the flow direction is larger than that expected by the bubble expansion. Thus, it can be seen that the bubble coalescence and breakup efficiency play an important role in the interfacial area transport. Excellent agreement was obtained between predicted and measured interfacial area concentrations.

3.4. Comparison of measured interfacial area concentration with derived model

All of measured interfacial area concentrations are compared with the interfacial area transport equation with the modeled sink and source terms. Figs. 8 and 9 show the results for the experiments in 25.4 and 50.8 mm diameter round tubes, respectively. In the figures, solid lines indicate the predicted interfacial area concentrations. Axial changes of the interfacial area concentrations can be reproduced by the interfacial area transport equation with the derived sink and source terms. The present model can predict almost all of data reasonably well as shown in Fig. 10. The average relative deviation between predicted and measured interfacial area concentrations is estimated to be 11.6%. It is recognized that the present model would

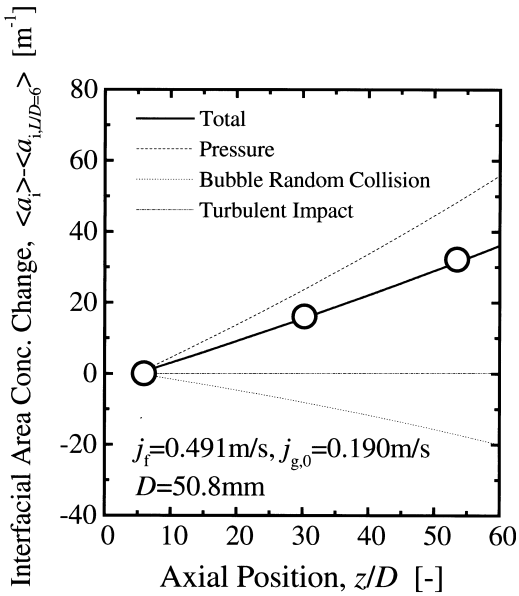

Fig. 4. Contributions of bubble coalescence, breakup and expansion to interfacial area transport ($j_f = 0.491$ m/s, $j_{g,0} = 0.190$ m/s).

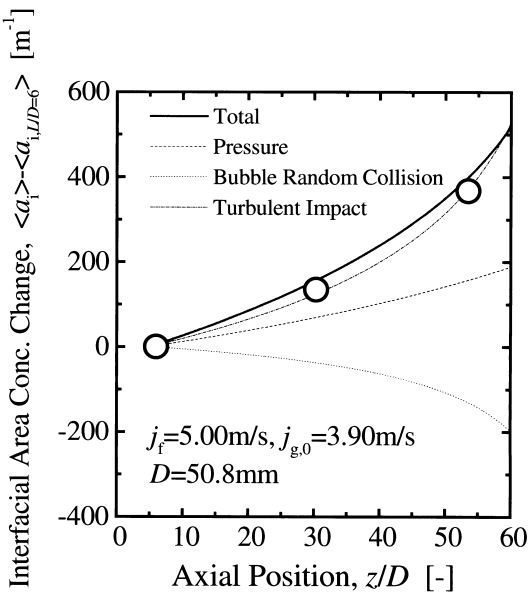

Fig. 5. Contributions of bubble coalescence, breakup and expansion to interfacial area transport ($j_f = 5.00$ m/s, $j_{g,0} = 3.90$ m/s).

be promising for the interfacial area transport of the examined bubbly flows (0.0414 m/s $\leq j_{g,0} \leq$ 3.90 m/s, 0.262 m/s $\leq j_f \leq$ 5.00 m/s, $1.27\% \leq \alpha \leq 46.8\%$, $D = 25.4$ mm, 50.8 mm). However, in the region near the bubbly to slug flow transition boundary, the introduction of the two-group interfacial area transport equation may be necessary to explain the phenomena. In the region, another interfacial area transport mechanisms such as bubble coalescence due to wake entrainment, and bubble breakup due to shearing-off and interfacial instability would be needed to be taken into account as the sink and source terms in the interfacial area transport equation. It should be pointed out that the applicability of the present model to other fluid systems, or smaller or larger diameter tubes should be examined experimentally, which means that the coefficients in this model, Γ_B, Γ_C, K_B, and K_C, should be modified by taking account of the rigorous data base taken in other fluid systems, or smaller or larger diameter tubes.

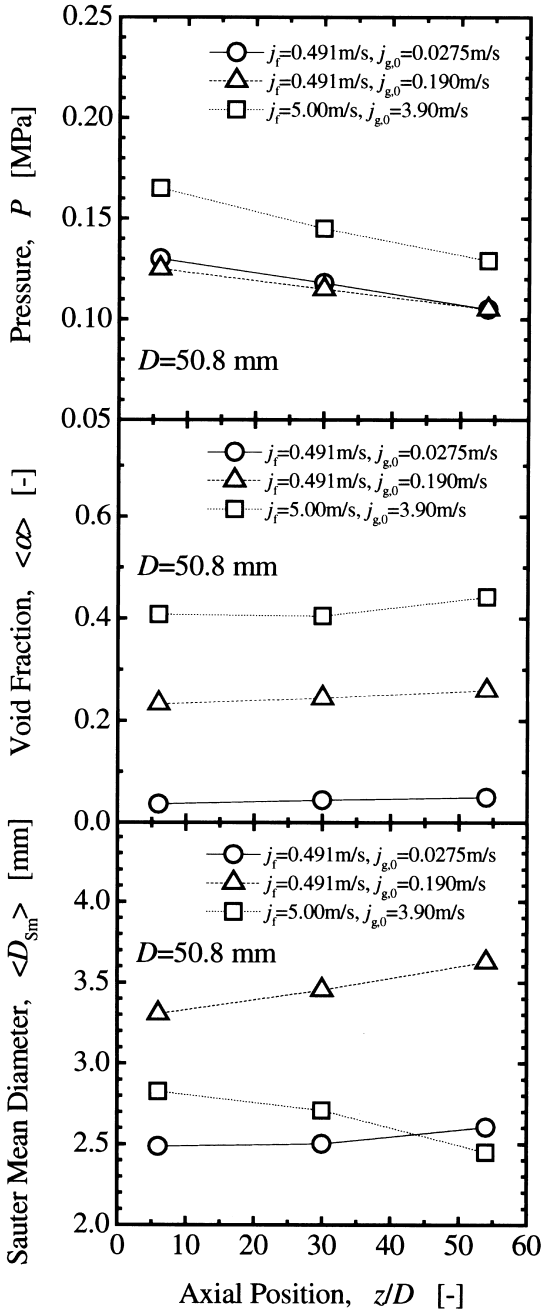

Fig. 6. Axial change of system pressure, void fraction, and Sauter mean diameter.

4. Conclusions

In relation to the development of the interfacial area transport equation, the sink and source terms in an adiabatic bubbly flow system were modeled based on the mechanisms of bubble–bubble and bubble–turbulent eddy random collisions, respectively. One-dimensional interfacial area transport equation with the derived sink and source terms was evaluated by using the area averaged flow parameters of adiabatic air-water bubbly flows measured in 25.4 mm and 50.8 mm diameter tubes. The flow conditions of the data set covered most of the bubbly flow regime, including finely dispersed bubbly flow. The following results were obtained:

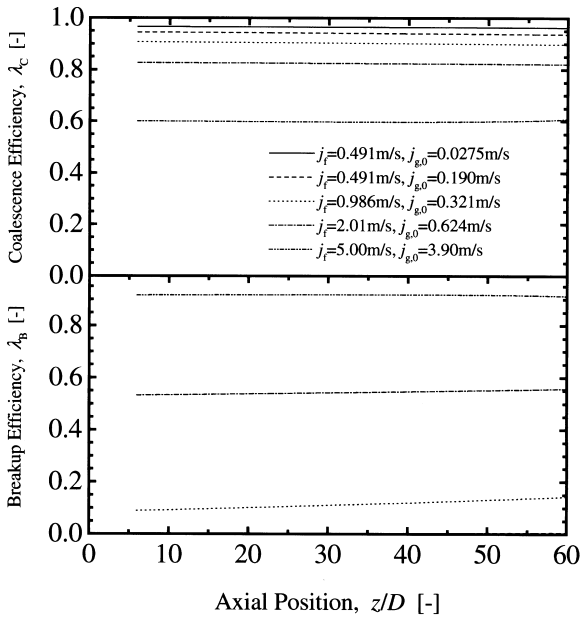

Fig. 7. Dependence of coalescence and breakup efficiency on gas and liquid velocities.

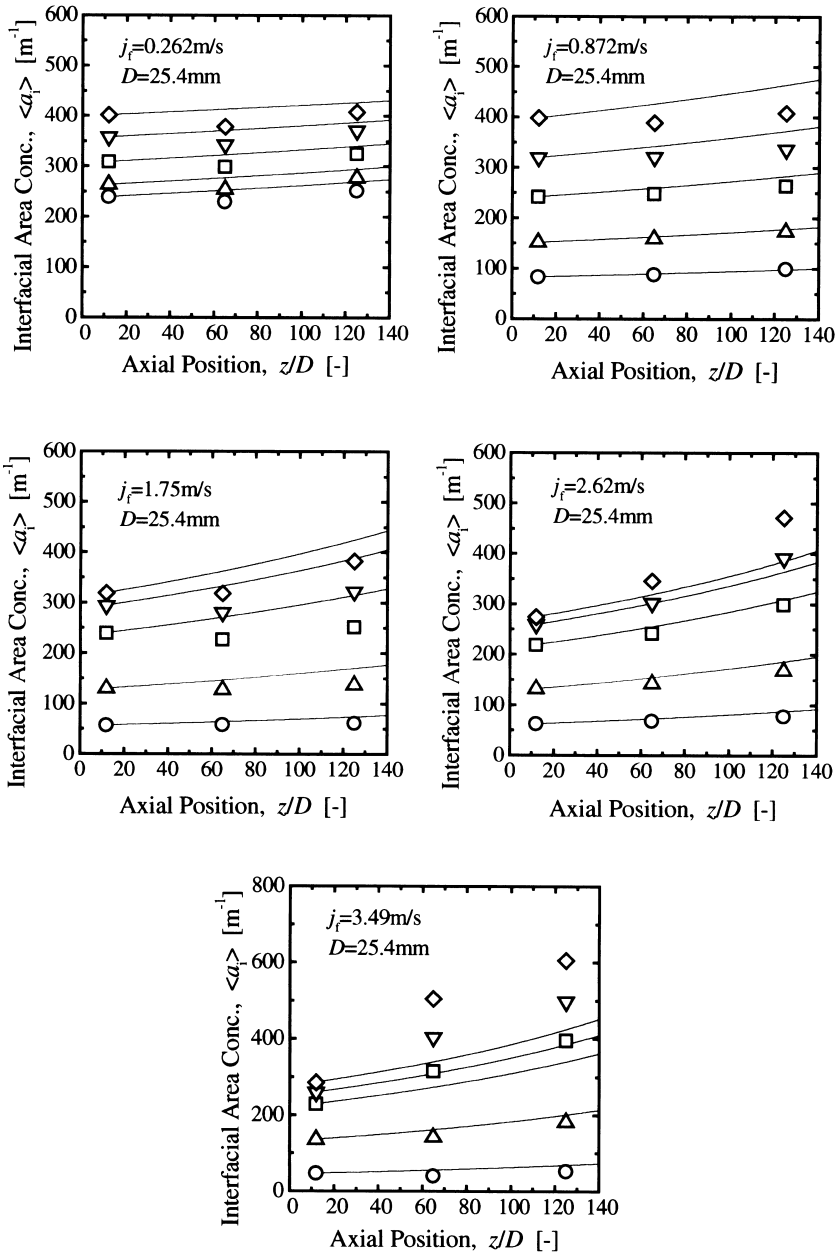

Fig. 8. Prediction of axial change of area averaged interfacial area concentration measured in 25.4 mm diameter tube by one-dimensional interfacial area transport equation with modeled sink and source terms.(a) $j_f = 0.262$ m/s, (b) $j_f = 0.872$ m/s, (c) $j_f = 1.75$ m/s, (d) $j_f = 2.62$ m/s, (e) $j_f = 3.49$ m/s

1. For relatively low liquid velocity and low void fraction, the bubble random collision and the turbulent impact might not contribute to the interfacial area transport significantly, whereas the bubble expansion due to pressure reduction along the axial direction was dominant for the interfacial area transport.
2. For relatively low liquid velocity and high void fraction, total change of the interfacial area concentration was smaller than that expected by the bubble expansion. This might be explained by the bubble breakup efficiency. Although the increase of the void fraction promoted the bubble random collision and the turbulent impact, the eddy might not have enough energy to disintegrate the bubbles. Consequently, the increase of the interfacial area concentration due to bubble breakup was negligible,

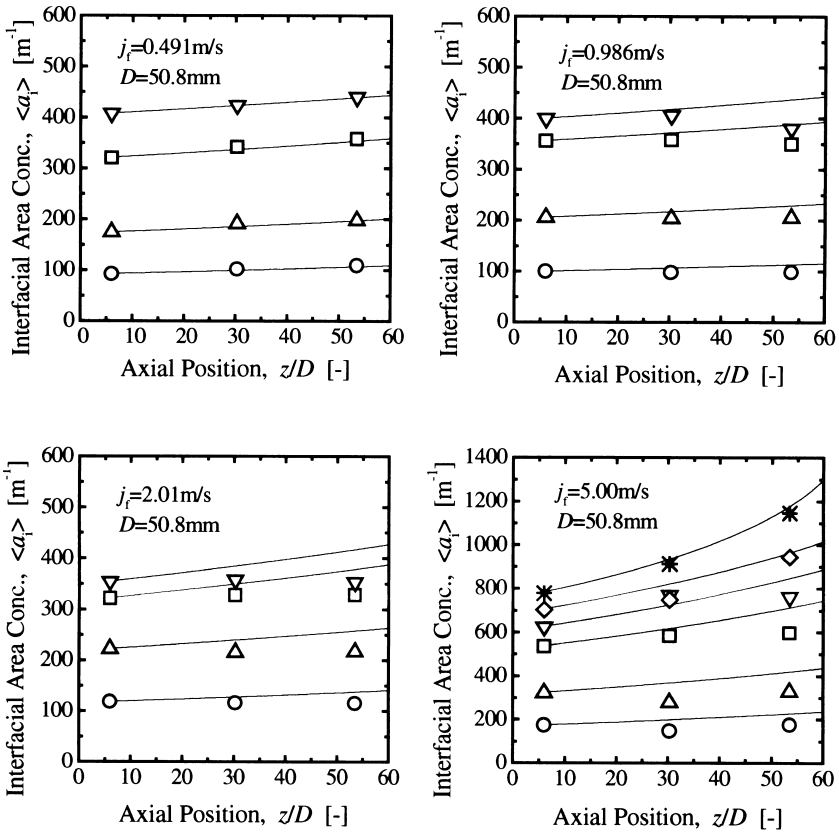

Fig. 9. Prediction of axial change of area averaged interfacial area concentration measured in 50.8 mm diameter tube by one-dimensional interfacial area transport equation with modeled sink and source terms.(a) $j_f = 0.491$ m/s, (b) $j_f = 0.986$ m/s, (c) $j_f = 2.01$ m/s, (d) $j_f = 5.00$ m/s

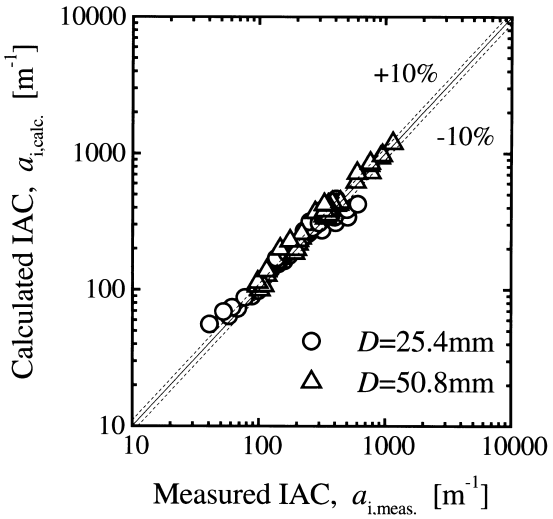

Fig. 10. Comparison between measured and predicted interfacial area concentrations.

whereas the decrease of the interfacial area concentration due to bubble coalescence was gradually enhanced along the flow direction, resulting in the increase of the interfacial area concentration along the flow direction.

3. For finely dispersed bubbly flow, the strong turbulence disintegrated bubbles into small bubbles, resulting in the increase of the interfacial area concentration. Although the strong turbulence increased the bubble collision rate, it might decrease the bubble contact time, resulting in the decrease of the bubble coalescence efficiency. As a result, the bubble breakup rate became higher than the bubble coalescence rate.
4. Excellent agreement was obtained between modeled and measured interfacial area concentrations within the average relative deviation of 11.6%. It was recognized that the present model would be promising for the interfacial area transport of the examined bubbly flows including the finely dispersed bubbly flows (0.0414 m/s $\leq j_{g,0} \leq$ 3.90 m/s, 0.262 m/s $\leq j_f \leq$ 5.00 m/s, 1.27% $\leq \alpha \leq$ 46.8%, $D = 25.4$ mm, 50.8 mm).

Acknowledgements

The authors would like to acknowledge Prof. Wu (Oregon State Univ., USA) and Prof. Tomiyama (Kobe Univ., Japan) for their valuable discussions. This work was performed under the auspices of the US Department of Energy's Office of Basic Energy Science. The authors would like to express their sincere appreciation for the encouragement, support and technical comments on this program from Drs. Manley, Goulard, and Price of DOE/BES.

References

[1] M. Ishii, K. Mishima, Study of two-fluid model and interfacial area. Technical report. ANL-80-111, Argonne National Laboratory, Chicago, IL, USA (1980).
[2] M. Ishii, Thermo-fluid dynamic theory of two-phase flow, Collection de la Direction des Etudes et Researches d'Electricité de France, Eyrolles, Paris, France, 22 (1975).
[3] G. Kocamustafaogullari, M. Ishii, Interfacial area and nucleation site density in boiling systems, International Journal of Heat and Mass Transfer 26 (1983) 1377.
[4] J.N. Reyes, Statistically derived conservation equations for fluid particle flows, in: Proceedings of ANS Winter Meeting, San Francisco, CA, USA, 1989, p. 12.
[5] G. Kocamustafaogullari, M. Ishii, Foundation of the interfacial area transport equation and its closure relations, International Journal of Heat and Mass Transfer 38 (1995) 481.
[6] C.A. Coulaloglou, L.L. Tavlarides, Description of interaction processes in agitated liquid–liquid dispersions, Chemical Engineering Science 32 (1977) 1289.
[7] M.J. Prince, H.W. Blanch, Bubble coalescence and break-up in air-sparged bubble columns, AIChE Journal 36 (1990) 1485.
[8] A.Y. Lafi, J.N. Reyes, Jr., Phenomenological models for fluid particle coalescence and breakage. Technical report, OSU-NE-9120, Department of Nuclear Engineering, Oregon State University, Corvallis, OR (1991).
[9] C. Tsouris, L.L. Tavlarides, Breakage and coalescence models for drops in turbulent dispersions, AIChE Journal 40 (1994) 395–406.
[10] Q. Wu, S. Kim, M. Ishii, S.G. Beus, One-group interfacial area transport in vertical bubbly flow, in: National Heat Transfer Conference, HTC-Vol.10, Baltimore, Maryland, 1997, p. 67.
[11] Q. Wu, S. Kim, M. Ishii, S.G. Beus, One-group interfacial area transport in vertical bubbly flow, International Journal of Heat and Mass Transfer 41 (1998) 1103.
[12] A. Kashyap, M. Ishii, S.T. Revankar, An experimental and numerical analysis of structural development of two-phase flow in a pipe. Technical report, PU-NE-94/2, School of Nuclear Engineering, Purdue University, West Lafayette, IN, 1994.
[13] T. Hibiki, S. Hogsett, M. Ishii, Local measurement of interfacial area, interfacial velocity and liquid turbulence in two-phase flow. Proceedings of OECD/CSNI Specialist Meeting on Advanced Instrumentation and Measurement Techniques, Santa Barbara, USA, Session IV, 1997, also in Nuclear Engineering and Design, 184 (1998) 287.
[14] T. Hibiki, M. Ishii, Z. Xiao, Local flow measurements of vertical upward air–water flow in a round tube, in: Proceedings of Third International Conference on Multiphase Flow, Lyon, France, 1998.
[15] T. Hibiki, M. Ishii, Axial development of liquid turbulence and interfacial area in bubbly two-phase flow. Proceedings of 1999 ASME-JSME Thermal Engineering Joint Conference, San Diego, CA, USA, 1999, also in International Journal of Heat and Mass Transfer, 42 (1999) 3019.
[16] H. Städtke, A. Blahak, B. Worth, Modelling of transport of interfacial area concentration in two-phase flow systems, in: Proceedings of Eighth International Topical Meeting on Nuclear Reactor Thermal-Hydraulics, vol.1, Kyoto, Japan, 1997, p. 69.
[17] L.B. Loeb, The Kinetic Theory of Gases, Dover, New York, USA, 1927.
[18] J.C. Rotta, Turbulence Stromungen, B.G. Teubner, Stuttgart, Germany, 1972.
[19] G. Kocamusfatafaogullari, W.D. Huang, J. Razi, Measurement of modeling of average void fraction, bubble size and interfacial area, Journal of Nuclear Engineering and Design 148 (1994) 437.
[20] Y. Taitel, D. Bornea, A.E. Dukler, Modelling flow pattern transitions for steady upward gas–liquid flow in vertical tubes, AIChE Journal 26 (1980) 345–354.
[21] T. Oolman, H.W. Blanch, Bubble coalescence in air-sparged bioreactors, Biotechnique Bioengineering 28 (1986) 578.
[22] T. Oolman, H.W. Blanch, Bubble coalescence stagnant liquids, Chemical Engineering Communication 43 (1986) 237.
[23] R.D. Kirkpatrick, M.J. Lockett, The influence of approach velocity on bubble coalescence, Chemical Engineering Science 29 (1974) 2363.
[24] W.K. Kim, K.L. Lee, Coalescence behavior of two bubbles in stagnant liquids, Journal of Chemical Engineering, Japan 20 (1987) 449.
[25] V.G. Levich, Physicochemical Hydrodynamics, Prentice-Hall, Englewood Cliffs, USA, 1962.
[26] D. Azbel, I.L. Athanasios, A mechanism of liquid entrainment, in: N. Cheremisinoff (Ed.), Handbook of Fluids in Motion, Ann Arbor Science Publishers, Ann Arbor, USA, 1983.
[27] D. Azbel, Two-phase flows in chemical engineering, Cambridge University Press, Cambridge, UK, 1981.
[28] S.T. Revankar, M. Ishii, Local interfacial area measurement in bubbly flow, International Journal of Heat and Mass Transfer 35 (1992) 913.
[29] A. Serizawa, I. Kataoka, Phase distribution in two-phase flow, in: N.H. Afgan (Ed.), Transient Phenomena in Multiphase Flow, Hemisphere, New York, USA, 1988, p. 179.
[30] R.W. Lockhart, R.C. Martinelli, Proposed correlation

of data for isothermal two-phase, two-component flow in pipes, Chemical Engineering Progress 5 (1949) 39.

[31] M. Ishii, One-dimensional drift–flux model and constitutive equations for relative motion between phases in various two-phase flow regimes. Technical report. ANL-77-47, Argonne National Laboratory, Chicago, IL, USA (1977).

[32] D. Chisholm, A theoretical basis for the Lockhart–Martinelli correlation for two-phase flow, International Journal of Heat and Mass Transfer 10 (1967) 1767.